tvst
Retina

Photoreceptor Layer Thinning as Biomarker for Circulatory Premature Mortality: UK Biobank Cohort Study

Mayinuer Yusufu[1,2], Mengtian Kang[3], Alimu Dayimu[4], Danli Shi[5–7], Lisa Zhuoting Zhu[1,2], Ruiye Chen[1,2], Algis J. Vingrys[8], Xianwen Shang[1,2,5,9], Mingguang He[5–7], and Lei Zhang[10–13]

[1] Centre for Eye Research Australia, Royal Victorian Eye and Ear Hospital, East Melbourne, Victoria, Australia
[2] Department of Surgery (Ophthalmology), The University of Melbourne, Melbourne, Parkville, Victoria, Australia
[3] Beijing Tongren Eye Center, Beijing Tongren Hospital, Capital Medical University, Dongcheng, Beijing, China
[4] Department of Oncology, University of Cambridge, Robinson Way, Cambridge, UK
[5] School of Optometry, The Hong Kong Polytechnic University, Hung Hom, Kowloon, Hong Kong, China
[6] Research Centre for SHARP Vision, The Hong Kong Polytechnic University, Hung Hom, Kowloon, Hong Kong, China
[7] Centre for Eye and Vision Research (CEVR), Hong Kong, China
[8] Department of Optometry & Visions Sciences, The University of Melbourne, Melbourne, Parkville, Victoria, Australia
[9] Guangdong Eye Institute, Department of Ophthalmology, Guangdong Provincial People's Hospital, Guangdong Academy of Medical Sciences, Guangzhou, Guangdong, China
[10] China-Australia Joint Research Center for Infectious Diseases, School of Public Health, Xi'an Jiaotong University Health Science Center, Xi'an, Shaanxi, PR China
[11] Phase I Clinical Trial Research Ward, The Second Affiliated Hospital of Xi'an Jiaotong University, Xi'an, Shaanxi Province, PR China
[12] Artificial Intelligence and Modelling in Epidemiology Program, Melbourne Sexual Health Centre, Alfred Health, Melbourne, Australia
[13] School of Translational Medicine, Faculty of Medicine, Nursing and Health Sciences, Monash University, Melbourne, Australia

Correspondence: Lei Zhang, China-Australia Joint Research Center for Infectious Diseases, School of Public Health, Xi'an Jiaotong University Health Science Center, Xi'an, Shaanxi 710061, PR China. e-mail: lei.zhang1@monash.edu
Mingguang He, Centre for Eye and Vision Research (CEVR), 17W Hong Kong Science Park, Hong Kong, China. e-mail: mingguang.he@polyu.edu.hk
Xianwen Shang, The Hong Kong Polytechnic University, 11 Yuk Choi Rd., Hung Hom, Kowloon, Hong Kong, China. e-mail: xianwen.shang@polyu.edu.hk

Received: March 20, 2025
Accepted: June 5, 2025
Published: August 5, 2025

Keywords: optical coherence tomography; all-cause mortality; circulatory mortality; premature mortality; cohort study

Purpose: To explore associations between optical coherence tomography (OCT) parameters and mortality risk.

Methods: This study used data from the UK Biobank participants with eligible OCT data. Feature selection was conducted with the least absolute shrinkage and selection operator. Selected parameters were fitted into Cox regression, with the full model adjusting for demographic, socioeconomic, lifestyle, and genetic factors.

Results: During a median follow-up duration of 10.6 years, 3174 were deceased. After matching the deceased and surviving participants (1:3) by age and gender, 12,696 were included. Ten out of 18 parameters showed significant associations with all-cause mortality. Each standard deviation increase in optic disc diameter parameters (hazard ratios [HRs] ranging from 1.042 to 1.052), thinning of ganglion cell-inner plexiform layer (HR = 0.958, 0.920–0.998), thinning of the photoreceptor layer and its sublayers (HRs = 0.937–0.960) were significant biomarkers of all-cause mortality. Cause-specific analyses by mortality age revealed that thinner photoreceptor layer and sublayers were significantly associated with circulatory premature mortality (HRs = 0.856–0.915).

Conclusions: Enlarging disc diameter, thinning of ganglion cell-inner plexiform layer, and thinning of photoreceptor layers are associated with all-cause mortality, with photoreceptor thinning especially linked to premature circulatory mortality.

Translational Relevance: These findings suggest that specific OCT parameters could serve as noninvasive biomarkers for mortality risk assessment, potentially enhancing early identification of individuals at higher risk of premature death, particularly from circulatory diseases.

Citation: Yusufu M, Kang M, Dayimu A, Shi D, Zhu LZ, Chen R, Vingrys AJ, Shang X, He M, Zhang L. Photoreceptor layer thinning as biomarker for circulatory premature mortality: UK Biobank cohort study. Transl Vis Sci Technol. 2025;14(8):10, https://doi.org/10.1167/tvst.14.8.10

Introduction

Premature mortality, typically defined as death before a certain age threshold, remains a significant public health concern. Studies revealed that a significant proportion, nearly half even in developed countries,[1,2] of premature mortality can be attributed to preventable factors. A previous meta-analysis[3] showed that simple behavioral factors, such as physical inactivity, smoking, and high alcohol intake, account for over half of all avoidable deaths. With early intervention, the individuals at higher risk could live a longer and healthier life. To bridge the gap between medical advances in preventive care and their practical implementation, one crucial requirement is the ability to accurately identify individuals at higher risk for premature mortality.

Nevertheless, previous studies on mortality prediction have predominantly concentrated on overall mortality.[4–7] In addition, whereas previous studies reviewed risk factors associated with premature mortality, they cannot be used as suitable biomarkers for risk assessment, because some are major health events rather than monitorable indicators, or they were obtained in specific patient groups rather than the general population or necessitate prolonged monitoring to capture meaningful temporal trends.[8–11] Thus identifying biomarkers that could be collected with a single noninvasive examination could empower healthcare professionals to proactively identify at-risk individuals and undertake targeted preventive measures.

Optical coherence tomography (OCT), as a noninvasive imaging technique, allows the identification of subtle changes in retinal structure to provide an opportunity for early intervention in the disease process.[12] For example, thinning of the ganglion cell layer, as measured by OCT, has been associated with an increased risk of cognitive decline and dementia.[13,14] Similarly, photoreceptor degenerations have been associated with brain and musculoskeletal diseases.[15]

Although previous studies have reported associations between OCT parameters and systemic conditions, research specifically targeting OCT parameters and mortality risk has been relatively limited. We hypothesize that OCT parameters may be associated with mortality risk. In this study, we aim to investigate the association between OCT parameters and the risk of all-cause and cause-specific mortality, as well as premature mortality.

Methods

Study Population

We used data from the UK Biobank, a large prospective cohort study, and STROBE (STrengthening the Reporting of OBservational studies in Epidemiology) guidelines were followed.[16] The baseline enrollment was from 2006 to 2010, and participants aged 40 to 69 years and registered with the National Health Service were enrolled. The study collected a vast array of data, including medical histories, lifestyle factors, genetics, and biomarkers through self-reported questionnaires, physical examinations, and tests. Detailed information regarding the study can be found elsewhere.[17]

In 2009, eye examinations were introduced and around 60,000 participants from six assessment centers underwent a baseline eye examination between 2009 and 2010, with a further 20,000 participants receiving eye assessments between 2012 and 2013.[18] Our study only included participants with OCT data.

Ascertainment of Mortality Data

Mortality data were linked through national death registries. The details of the data linkage procedure are available (https://biobank.ndph.ox.ac.uk/showcase/refer.cgi?id=115559). The date of the image acquisition was considered as the baseline and corresponding baseline covariates were used. The surviving participants were censored on December 31, 2020. In our study, the primary outcome was overall mortality (i.e., all deaths occurring during the follow-up). In addition, we further analyze the association between OCT parameters and premature mortality (i.e., deaths occurring during the follow-up and before the age of 75 years, the cut-off age for premature mortality in the United Kingdom).[19] The cause of death was determined using the Interna-

tional Classification of Diseases, edition 10. Because we are exploring the association between OCT parameters and mortality as indicators of systemic health, the participants who died from external causes (V01–Y89) were excluded (Supplementary Table S1).

Ascertainment of OCT Parameters

Spectral-domain OCT imaging was performed to obtain retinal scans in a dark room without pupil dilation, and the details have been previously published.[18] Specifically, the imaging protocol used a three-dimensional macular volume scan covering a 6 × 6 mm raster pattern, with a scan density of 512 horizontal A-scans per B-scan and 128 B-scans.[18] Segmentation of retinal layers was performed using the automated Topcon Advanced Boundary Segmentation (TABS)[20,21] algorithm (version 1.6.1.1) integrated into the Topcon 3D OCT-1000 Mark II software (Topcon Optical Company, Tokyo, Japan), which delineated retinal layers, including photoreceptor layers and sublayers, based on dual-scale gradient information. A total of 52 OCT parameters were extracted by previous researchers with TABS[20] and returned to UK Biobank, including 44 derived measures and 8 quality control measures[21] (Supplementary Table S2). The parameters included the thickness of Early Treatment Diabetic Retinopathy Study subfields, namely central subfield, which refers to a region with a diameter of 1 mm measured from the center of the fovea; inner subfield, which refers to the area located between 1 to 3 mm from the center of the fovea; and outer subfield, which refers to the area located between 3 to 6 mm from the center of the fovea. To ensure accuracy, quality control checks were implemented by using quality control measures and excluding eyes with conditions that would potentially affect the accuracy of segmentation following the same criteria used by authors that reported the value of OCT parameters.[22] First, based on quality control measures, we excluded those with image quality score <45, the poorest 20% centration certainty, or the poorest 20% segmentation certainty. Subsequently, participants with IOP of ≥22 mm Hg or ≤5 mm Hg, self-reported glaucoma or macular degeneration, and self-reported history of glaucoma surgery were also excluded.[22]

Covariates

Ethnicity, Townsend index, and education were included as potential demographic and socioeconomic confounders. Age, gender, and ethnicity data were retrieved from questionnaires. The Townsend index was used to indicate social deprivation, and education was classified into 3 levels: high, intermediate, and low.[23] Lifestyle covariates included smoking status (previous, current, never), alcohol consumption (previous, current, never), and physical activity (high, moderate, and low levels based on the International Physical Activity Questionnaire). The body mass index (BMI) was calculated by dividing an individual's weight in kilograms by the square of their height in meters. In addition, we further included the genetic risk score for longevity.[24]

Statistical Analysis

For continuous variables, the mean and standard deviation (SD) were used to represent the data, and for categorical variables, a percentage was used. The χ^2 test was used for categorical variables. For numerical variables, we conducted a *t*-test to assess intergroup differences in data that exhibited a normal distribution and, a Wilcoxon rank-sum test or Kruskal-Wallis test for data with a non-normal distribution.

First, OCT parameters with a missing proportion of > 30% were excluded, and the missing values were imputed using Random Forest (missForest package version 1.5). We rescaled data to SD units to better understand the association between one SD unit increase in OCT parameters and the change in mortality risk. Because of the relatively low number of deaths compared to the total number of participants, a matching approach was employed. We matched each deceased individual with three surviving individuals from the dataset based on sex and age with a ratio of 1:3 using MatchIt package version 4.5.3, ensuring similarity in terms of age and gender to address the imbalanced nature of included participants and enhance the statistical power of the analysis.

We used the least absolute shrinkage and selection operator (LASSO) for feature selection. This technique systematically identifies the most predictive variables by shrinking less important feature coefficients to zero, thereby reducing dimensionality and mitigating the risk of false discoveries in the subsequent Cox regression analysis. After addressing the challenge of multiple testing through feature selection, selected OCT parameters were fitted into Cox proportional hazard regression. Hazard ratios (HRs) were used to quantify the effect size of each parameter. An HR > 1.0 indicates an increased hazard (i.e., higher risk of the outcome associated with an increase in the parameter value), while an HR < 1.0 indicates a decreased hazard (i.e.,

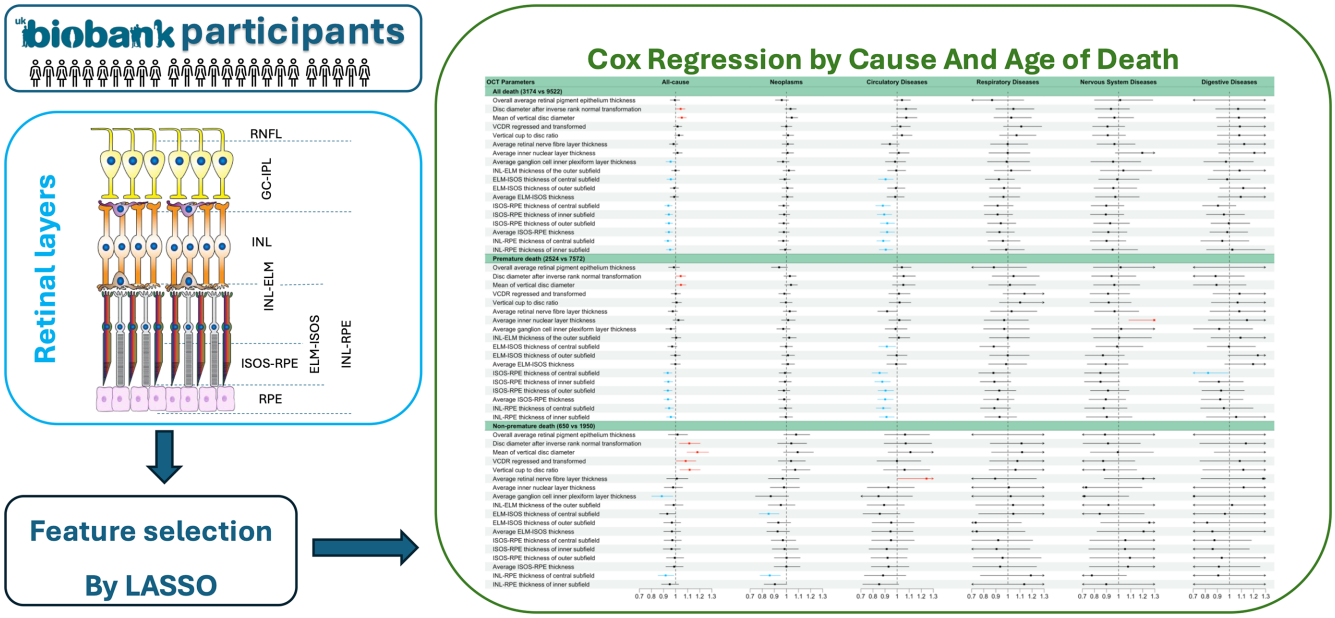

Figure 1. Study design. LASSO, Least Absolute Shrinkage and Selection Operator; RNFL, retinal nerve fiber layer. This figure used images from Elisa Galliano. Retina circuit. DOI: 10.5281/zenodo.4756818 from SciDraw and Chilton, J. (2020). Ependymal cell.Zenodo. https://doi.org/10.5281/zenodo.3926497 from SciDraw.

lower risk of the outcome associated with an increase in the parameter value). To validate the robustness of the associations, we incrementally added the covariates in the regression model: Model 1 adjusted with the False Discovery Rate method, and Model 2 adjusted for demographic factors, including ethnicity, Townsend index (social deprivation), and education. Model 3 further controlled lifestyle and health factors (body mass index, smoking, alcohol, and physical activity). Model 4 was adjusted for Model 3 plus the genetic risk score.

Figure 1 shows the study design. The results of subgroup analyses and sensitivity analyses are presented in Supplementary Tables S3–S10. Statistical significance was defined as a two-tailed *P* value of 0.05. R 4.2.3 was used to perform all statistical analyses.

Results

Baseline Demographic Characteristics

A total of 84,414 participants who had OCT examinations were assessed for eligibility, and 70,903 were included (Fig. 2). During a median follow-up period of 10.6 years (interquartile range [IQR] 10.5∼10.79), 3,174 were deceased, with 2524 premature deaths. The median follow-up time was 6.40 years (IQR 4.2∼8.6) for premature deaths and 9.15 years (IQR 7.6∼10.3) for non-premature deaths.

After matching by age and gender, the final analysis included a total of 12,696 participants, with 9522 surviving and 3174 deceased participants and a median follow-up of 10.6 years (IQR 8.09∼10.74). Significant differences in socioeconomic and health-related factors were observed between surviving and deceased participants. The deceased participants had a significantly higher mean BMI, lower levels of physical activity, and higher proportions of smoking and alcohol consumption than the surviving participants (all $P < 0.001$). A significantly higher level of social deprivation (measured by the Townsend Index) and a lower education level were also found for the deceased participants (all $P < 0.001$) (Table).

Association Between OCT Parameters and Overall Mortality

After removing parameters with more than 30% missing data and feature selection with LASSO, 18 parameters were included in the Cox regression models. Supplementary Table S11 presents detailed descriptive measurements.

In the fully adjusted model, 10 out of 18 parameters remained significantly associated with all-cause mortality. Larger mean vertical disc diameter (DD) and DD after inverse rank normal transformation were associated with increased mortality risk, with an HR of 1.052 (95% confidence interval [CI],

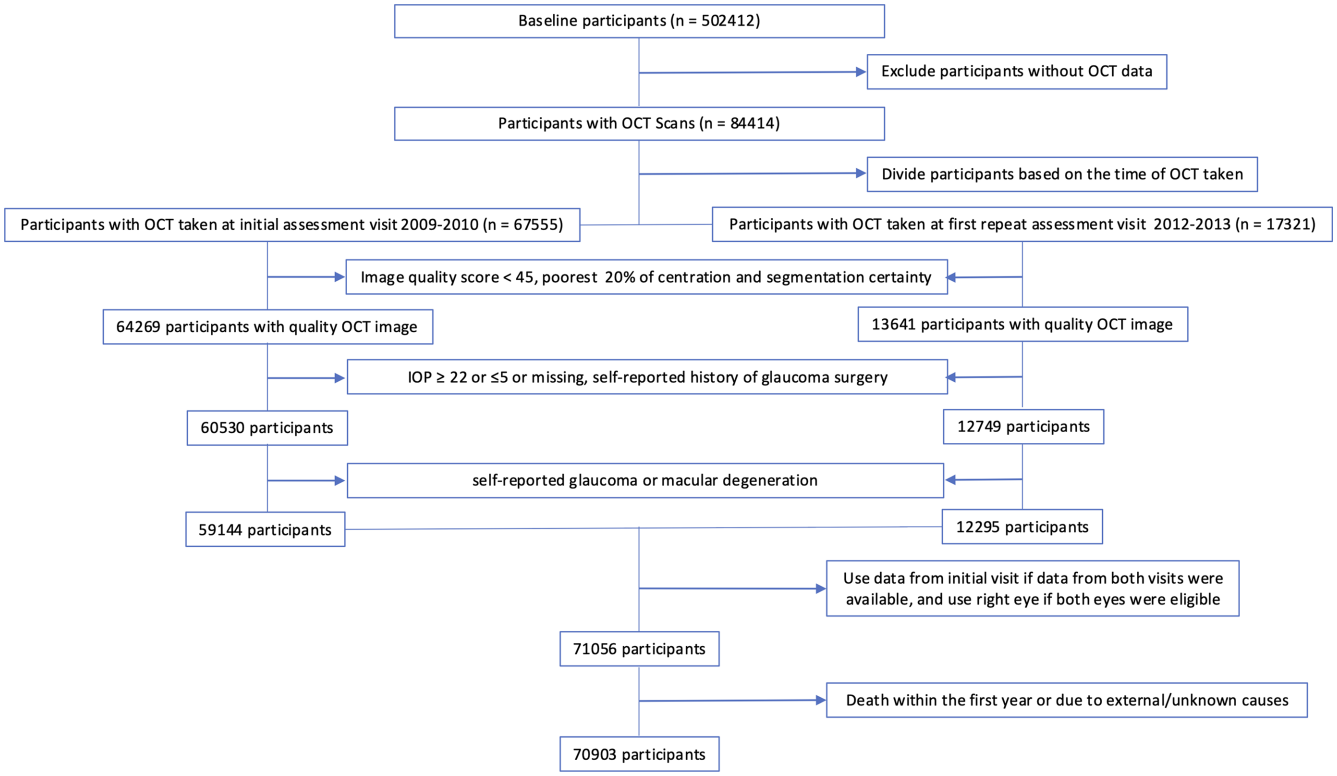

Figure 2. Participants selection process.

1.015–1.090) and 1.042 (CI, 1.006–1.079), respectively. Conversely, the thinning of the ganglion cell-inner plexiform layer (GC-IPL) demonstrated an association with increased risk, with an HR of 0.958 (CI, 0.920–0.998). In addition, the thinning of seven photoreceptor layers and sublayers was also associated with elevated all-cause mortality risk, with the HRs ranging from 0.937 (CI, 0.907–0.967) and 0.955 (CI, 0.924–0.988) for the central and inner subfields of inner nuclear layer-RPE (INL-RPE), 0.960 (CI, 0.928–0.994) for the central subfield thickness of external limiting membrane-inner segment outer segment (ELM-ISOS), 0.944 (CI, 0.914–0.975) for the average thickness of ISOS-RPE, and 0.940 (CI, 0.910–0.972), 0.944 (CI, 0.913–0.976), and 0.944 (CI, 0.914–0.976) for its central, inner and outer subfields (Fig. 3).

Further analysis of the causes of death showed that seven photoreceptor sublayers of the 10 parameters exhibited the same associations with circulatory mortality, with HR ranging from 0.883 to 0.918. Although multiple OCT parameters were associated with circulatory mortality, they did not show a significant association with mortality caused by other major diseases, including neoplasms, respiratory diseases, digestive diseases, and nervous system diseases (Fig. 4).

Association Between OCT Parameters and Premature Mortality

In the fully adjusted model, eight parameters showed significant association with all-cause premature mortality. Larger mean vertical DD (1.044; CI, 1.003–1.088) and DD after inverse rank normal transformation (1.042; CI, 1.002–1.084) were only significantly associated with increased all-cause premature mortality risk, and the associations were not found for cause-specific premature mortality. In addition, each SD decrease in central and inner subfields of INL-RPE was associated with HRs of 0.947 (CI, 0.913–0.983) and 0.961 (CI, 0.925–0.998) for all-cause premature mortality risk. HR for thinning of the average thickness of ISOS-RPE and its central, inner, and outer subfields was 0.937 (CI, 0.903–0.972), 0.935 (CI, 0.901–0.971), 0.940 (CI, 0.906–0.976), and 0.936 (CI, 0.902–0.970), respectively (Fig. 3).

For cause-specific premature mortality, the thinning of seven photoreceptor layer-related parameters was significantly associated with increased premature mortality risk from circulatory diseases. HR for premature circulatory mortality risk was 0.887 (CI, 0.828–0.949) and 0.913 (CI, 0.853–0.977) for INL-RPE central and inner subfields, 0.915 (CI, 0.848–0.987) for ELM-ISOS central subfield, 0.901 (CI, 0.839–0.968)

Table. Baseline Characteristics of Participants

	All (N = 12,696)	Surviving (N = 9522)	Deceased (N = 3174)	*P* Value	Premature Mortality (N = 2524)	Non-Premature Mortality (N = 650)	*P* Value
Age, mean (SD)	62.4 (6.26)	62.4 (6.26)	62.4 (6.26)	1.00	60.9 (6.05)	68.4 (2.20)	**<0.001**
Sex							
Female	5320 (41.9%)	3990 (41.9%)	1330 (41.9%)	1.00	1090 (43.2%)	240 (36.9%)	**0.005**
Male	7376 (58.1%)	5532 (58.1%)	1844 (58.1%)		1434 (56.8%)	410 (63.1%)	
Ethnicity							
White	11887 (93.6%)	8924 (93.7%)	2963 (93.4%)	**0.042**	2348 (93.0%)	615 (94.6%)	0.91
Mixed	62 (0.5%)	50 (0.5%)	12 (0.4%)		10 (0.4%)	2 (0.3%)	
Asian	295 (2.3%)	235 (2.5%)	60 (1.9%)		50 (2.0%)	10 (1.5%)	
Black	237 (1.9%)	163 (1.7%)	74 (2.3%)		61 (2.4%)	13 (2.0%)	
Other	126 (1.0%)	91 (1.0%)	35 (1.1%)		29 (1.1%)	6 (0.9%)	
Townsend index, mean (SD)	−1.29 (2.94)	−1.45 (2.86)	−0.824 (3.13)	**<0.001**	−0.791 (3.15)	−0.951 (3.05)	0.24
Education level							
High	4097 (32.3%)	3239 (34.0%)	858 (27.0%)	**<0.001**	691 (27.4%)	167 (25.7%)	**<0.001**
Intermediate	6027 (47.5%)	4518 (47.4%)	1509 (47.5%)		1244 (49.3%)	265 (40.8%)	
Low	2401 (18.9%)	1642 (17.2%)	759 (23.9%)		551 (21.8%)	208 (32.0%)	
BMI, mean (SD)	27.5 (4.61)	27.3 (4.34)	28.2 (5.27)	**<0.001**	28.2 (5.38)	28.1 (4.86)	0.62
Smoking status							
Never	6267 (49.4%)	4997 (52.5%)	1270 (40.0%)	**<0.001**	987 (39.1%)	283 (43.5%)	**<0.001**
Previous	5151 (40.6%)	3799 (39.9%)	1352 (42.6%)		1061 (42.0%)	291 (44.8%)	
Current	1190 (9.4%)	663 (7.0%)	527 (16.6%)		455 (18.0%)	72 (11.1%)	
Alcohol consumption							
Never	525 (4.1%)	354 (3.7%)	171 (5.4%)	**<0.001**	125 (5.0%)	46 (7.1%)	0.075
Previous	498 (3.9%)	308 (3.2%)	190 (6.0%)		156 (6.2%)	34 (5.2%)	
Current	11636 (91.7%)	8834 (92.8%)	2802 (88.3%)		2234 (88.5%)	568 (87.4%)	
Physical activity							
Low	1963 (15.5%)	1372 (14.4%)	591 (18.6%)	**<0.001**	487 (19.3%)	104 (16.0%)	**0.033**
Moderate	4194 (33.0%)	3186 (33.5%)	1008 (31.8%)		803 (31.8%)	205 (31.5%)	
High	4122 (32.5%)	3223 (33.8%)	899 (28.3%)		691 (27.4%)	208 (32.0%)	

SD, standard deviation.

Data were expressed as the mean (SD) for continuous variables or the percentage for category variables. For differences between groups, a *t*-test or Wilcoxon rank-sum test for numerical variables and chi-squared test for categorical variables were used. Premature mortality refers to the deaths that occur before the age of 75 years. Non-premature mortality refers to the deaths that occur at or after the age of 75 years.

for the average thickness of ISOS-RPE, and 0.856 (CI, 0.795–0.922), 0.878 (CI, 0.816–0.945), and 0.904 (CI, 0.842–0.971) for its central, inner, and outer subfields (Fig. 5).

Association Between OCT Parameters and Non-Premature Mortality

For non-premature all-cause mortality, both larger mean vertical DD (1.183; CI, 1.095–1.278) and DD after inverse rank normal transformation (1.115; CI, 1.030–1.206) showed significant associations, which was consistent with their association with overall and premature all-cause mortality. Thinning of GC-IPL (0.885; CI, 0.801–0.977) was also significantly associated with non-premature all-cause mortality but not cause-specific mortality. Moreover, no photoreceptor layer-related parameters showed significant associations with non-premature circulatory mortality (Figs. 3, 4).

Discussion

Premature mortality attributed to non-communicable diseases remains a critical global health concern, with the World Health Organization setting a target to reduce such fatalities by one-third by 2030

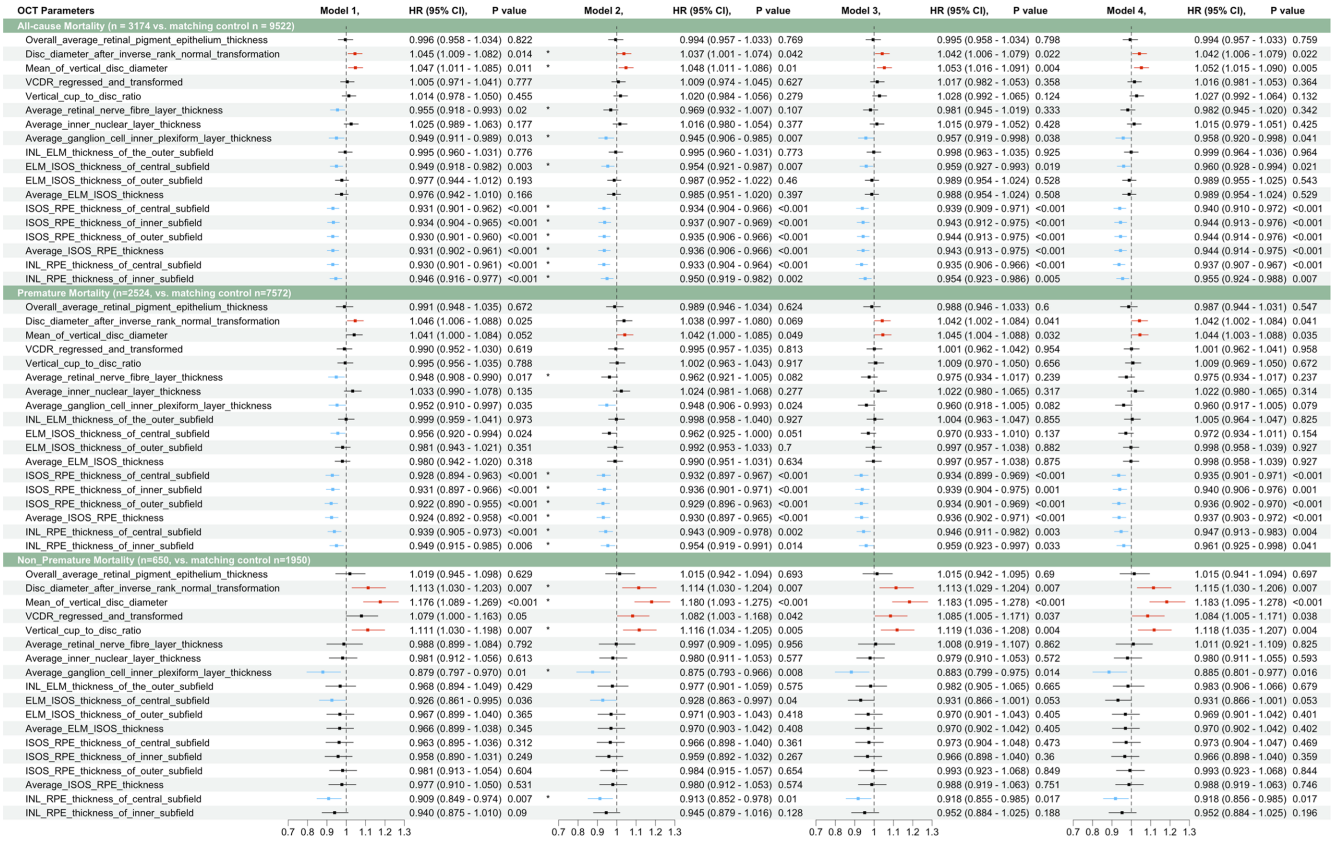

Figure 3. OCT parameters and their associations with all-cause mortality. This plot shows the hazard ratio associated with each standard deviation change in OCT parameters. *Asterisk* indicates false discovery rate (FDR) adjusted $P < 0.05$, VCDR, vertical cup-to-disc ratio. Model 1 was unadjusted, yet the *P* value was further adjusted with FDR. Model 2 included both OCT measurements and demographic factors, including ethnicity, Townsend index (social deprivation), and education. Model 3 used covariates from Model 2 and added lifestyle and health factors (BMI, smoking, alcohol, and physical activity). Model 4 was adjusted for Model 3 plus the genetic risk score.

as part of the Sustainable Development Goals. In this study, we investigated the association between OCT parameters and risk of mortality and premature mortality. We found that the thinning of the photoreceptor layer and sublayers were sensitive indicators for increased risk of premature mortality, especially premature mortality caused by circulatory diseases. The identification of these specific OCT parameters as early markers for heightened premature mortality risk has the potential to enable timely interventions and align with global health initiatives aiming to curb premature deaths from non-communicable diseases. In addition, larger DD and thinner GC-IPL were significantly associated with an increased risk of all-cause mortality.

Our study demonstrated that larger disc diameter and thinned GC-IPL could be strong indicators for increased all-cause mortality risk. The potential underlying mechanisms could be multifactorial, as further analysis of cause-specific mortality revealed no significant association between those parameters and mortality caused by other major diseases. Previous studies reported larger optic disc areas and thinner GC-IPL in patients with metabolic disorders and neurodegenerative conditions.[25–27] An increase in the OCT-determined DD and thinner GC-IPL may be the result of optic nerve head damage because of various causes, such as accumulation of advanced glycation end products[25] and aldosterone-induced vasculopathy,[26] and associated with demyelination in the central nervous system and ganglion cell loss induced by inflammatory demyelination.[28]

Our study revealed that the thinning of the photoreceptor layer and sublayers (INL-RPE, ELM-ISOS, and ISOS-RPE) were significantly associated with an increased risk of premature mortality due to circulatory diseases, but not with non-premature mortality. Although the associations were found for both all-cause mortality and circulatory disease-related mortality, further analysis of cause-specific mortality risk showed that the associations were mainly attributable to mortality due to circulatory diseases.

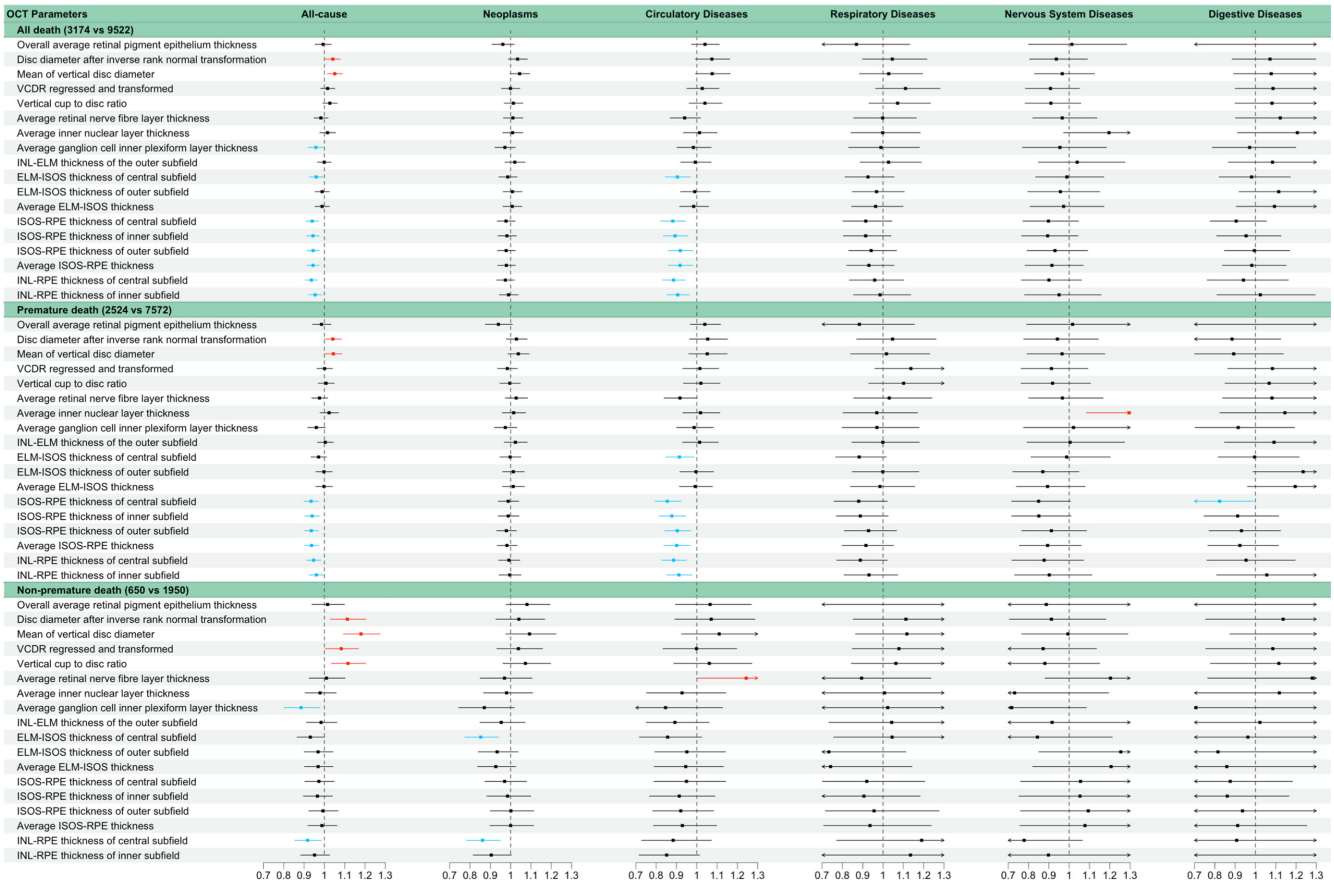

Figure 4. OCT parameters and their associations with mortality by cause in the multivariate model. This plot shows the hazard ratio associated with each standard deviation change in OCT parameters. VCDR, vertical cup-to-disc ratio. The multivariate model adjusted for demographic factors, including ethnicity, Townsend index (social deprivation), education, lifestyle, and health factors (BMI, smoking, alcohol, and physical activity) plus the genetic risk score.

OCT Parameters	All mortality	HR (95% CI)	P value	Premature mortality	HR (95% CI)	P value
Overall average retinal pigment epithelium thickness		1.039 (0.976 - 1.106)	0.235		1.038 (0.969 - 1.111)	0.29
Disc diameter after inverse rank normal transformation		1.075 (0.993 - 1.164)	0.075		1.054 (0.964 - 1.153)	0.248
Mean of vertical disc diameter		1.077 (0.993 - 1.168)	0.072		1.052 (0.961 - 1.152)	0.274
VCDR regressed and transformed		1.028 (0.950 - 1.111)	0.496		1.016 (0.929 - 1.110)	0.734
Vertical cup to disc ratio		1.041 (0.962 - 1.127)	0.322		1.021 (0.933 - 1.116)	0.657
Average retinal nerve fibre layer thickness		0.937 (0.861 - 1.019)	0.127		0.912 (0.830 - 1.003)	0.057
Average inner nuclear layer thickness		1.013 (0.938 - 1.093)	0.749		1.017 (0.936 - 1.106)	0.691
Average ganglion cell inner plexiform layer thickness		0.983 (0.902 - 1.072)	0.7		0.987 (0.900 - 1.083)	0.785
INL-ELM thickness of the outer subfield		0.992 (0.915 - 1.076)	0.854		1.015 (0.925 - 1.113)	0.753
ELM-ISOS thickness of central subfield		0.905 (0.845 - 0.968)	0.004		0.915 (0.848 - 0.987)	0.022
ELM-ISOS thickness of outer subfield		0.990 (0.920 - 1.066)	0.79		0.996 (0.917 - 1.082)	0.928
Average ELM-ISOS thickness		0.985 (0.916 - 1.059)	0.677		0.993 (0.914 - 1.077)	0.858
ISOS-RPE thickness of central subfield		0.883 (0.824 - 0.946)	<0.001		0.856 (0.795 - 0.922)	<0.001
ISOS-RPE thickness of inner subfield		0.894 (0.836 - 0.956)	0.001		0.878 (0.816 - 0.945)	<0.001
ISOS-RPE thickness of outer subfield		0.918 (0.861 - 0.980)	0.01		0.904 (0.842 - 0.971)	0.006
Average ISOS-RPE thickness		0.918 (0.860 - 0.980)	0.01		0.901 (0.839 - 0.968)	0.005
INL-RPE thickness of central subfield		0.887 (0.833 - 0.944)	<0.001		0.887 (0.828 - 0.949)	<0.001
INL-RPE thickness of inner subfield		0.907 (0.854 - 0.964)	0.002		0.913 (0.853 - 0.977)	0.009

Figure 5. OCT parameters and their associations with circulatory mortality in the multivariate model. Notes: This plot shows the hazard ratio associated with each standard deviation change in OCT parameters. VCDR, vertical cup-to-disc ratio. The multivariate model adjusted for demographic factors, including ethnicity, Townsend index (social deprivation), education, lifestyle, and health factors (BMI, smoking, alcohol, and physical activity) plus the genetic risk score.

translational vision science & technology

Specifically, these were associated with premature mortality due to circulatory diseases, as no significant association was found for non-premature circulatory mortality. Previous studies reported thinner INL-PRE in individuals with higher systolic blood pressure,[29] higher HbA1c and diabetes,[30] and smoking behavior.[31] In addition, the thinner ELM-ISOS sublayer was also found to be associated with higher systolic blood pressure and smoking.[29] High blood pressure and systemic toxicity due to smoking may have caused vascular damage, which leads to reduced blood flow and ischemia in retinal capillary layers, thereby leading to the thinning of INL-PRE.[32–34] Moreover, a thinner INL-PRE sublayer was also associated with less physical activity[31]. Studies have shown that regular physical exercise[35–37] could reduce inflammatory stimulation and oxidative stress on the circulatory system, hence physical inactivity may, to some extent, account for the association between a thinned photoreceptor layer and increased mortality risk caused by circulatory diseases. Previous research also revealed thinner ISOS-RPE sublayers in participants who smoke[29] or have diabetes.[38] As studies have shown, smoking and increased advanced glycation end products production would lead to the accumulation of toxicity, oxidative damage, and inflammation, which would result in microvascular damage and metabolic dysfunction.[27,31,39–42] Those pathological changes may have led to the reduced blood supply and accelerated apoptosis of the photoreceptor layer and its sublayers.

Overall, the evidence from previous studies may suggest that the thinning of the photoreceptor layer and sublayers may indicate the presence of vascular damage, oxidative stress, and inflammation, which may have contributed to the thinning and structural changes. McFarland and Fisher[43] have found that the absolute threshold of vision decreases with age and have attributed this to reduced oxygen tension at the PR consistent with a vascular mechanism.[44] This may partly explain the associations between the thinning photoreceptor layer and its sublayers with increased risk of mortality, especially circulatory disease-related mortality. Given the critical role of the photoreceptor layer and sublayers, more in-depth research leveraging advanced imaging technologies could provide additional insights. Especially, recent advancements in high-resolution OCT (<3 µm axial resolution) and review tool[45] have enabled finer delineation of retinal layers (28 retinal bands), with our INL-RPE thickness likely encompassing approximately 15 bands in their nomenclature. In addition, enhanced resolution and refined segmentation could further improve precision in detecting subtle sublayer changes and potentially strengthen associations with vascular pathology.

In addition, when further examining the subfields of photoreceptor layers (INL-RPE, ELM-ISOS and ISOS-RPE), central subfields of all three layers, inner subfields of INL-RPE and ISOS-RPE layers, and outer subfield of ISOS-RPE layer showed significant associations, indicating central subfield may hold more relevance for indicating increased risk of mortality due to circulatory diseases, followed by inner subfield, and then outer subfield. The central subfield, being near the fovea and representing an area of high metabolic activity and distant to direct retinal vascular supply,[46] could be more sensitive to microvascular damage or impaired oxygen and nutrient supply and thus may better reflect the overall health of the circulatory system. A previous study on age-related macular degeneration research demonstrated the fovea's resilience because of specialized protective mechanisms including enhanced macular pigment density, unique photoreceptor architecture, and alternative metabolic support pathways.[47] We believe that the observed associations between central field measurements and mortality, despite these well-established protective mechanisms, may indicate the severity of the underlying systemic pathological processes. The fact that mortality associations are detectable in a retinal region equipped with robust protective mechanisms may suggest that the systemic vascular or metabolic perturbations are sufficiently severe to overcome local protective mechanisms. Compared with the central subfield, as the inner subfield and outer subfield are located farther from the fovea and are supported by retinal vascular beds, they may not reflect changes in overall vascular health as effectively. In addition, changes in the central subfield have the greatest impact on visual acuity,[46] and previous studies have already shown that vision impairment increases mortality risk.[48] This may also explain the stronger associations found for changes in the central subfield compared with those in the inner and outer subfields.

The current study included a large sample size and examined a comprehensive range of OCT parameters, allowing for a detailed examination of retinal structure. Traditional assessment of retinal thickness as a surrogate for the function is limited, as retinas with neuronal loss or disrupted inner layers can have normal thickness due to extracellular fluid.[49] Our study addresses this limitation by examining specific sublayers, providing a more reliable association with mortality risk. After adjusting for demographic, socioeconomic, lifestyle, and genetic risk factors, we identified OCT parameters that could serve as indicators for overall

mortality risk and circulatory disease-related mortality risk independent of traditional risk factors. More importantly, our study revealed that the thinning of the photoreceptor layer and its sublayers could be a sensitive indicator for increased premature mortality risk.

However, it is important to note that our study only focused on associations with mortality outcomes, although our results were statistically significant, it does not indicate a causal relationship. Further research is needed to understand the underlying mechanisms linking changes in OCT parameters to systemic health and vascular integrity. In addition, the majority of the study population are of white ethnicity. Further study in other population groups is needed. Additionally, the systematic measurement discrepancies of the automated OCT segmentation algorithm would limit the absolute accuracy of individual measurements. However, this systematic bias does not affect the validity of our association analyses due to consistent offset across all participants and our measurement standardization approach. Another limitation of our study is the lack of direct assessment of choriocapillaris and Bruch's membrane thickness. Given that the outer retinal layers showing mortality associations are primarily supplied by the choroidal circulation, this limits our understanding of the vascular mechanisms potentially underlying our findings. Recent advances in high-resolution OCT segmentation algorithms have demonstrated the capability to assess these choroidal structures,[45] suggesting that future studies incorporating enhanced imaging techniques could provide deeper insights into the choroidal vascular contributions to retinal-systemic health relationships.

Conclusions

In summary, our findings highlight the significance of specific OCT parameters in assessing mortality risk, particularly concerning overall mortality and premature mortality attributed to circulatory diseases. Larger DD and thinner photoreceptor layers and GC-IPL could indicate the presence of systemic health conditions and a higher mortality risk. Particularly, the thinning of the photoreceptor layer and its sublayers was associated with an increased risk of premature mortality due to circulatory diseases. Further research is warranted to unravel the underlying mechanisms and establish the clinical utility of these OCT parameters in informing tailored preventive strategies.

Acknowledgments

The Centre for Eye Research Australia receives Operational Infrastructure Support from the Victorian State Government.

Supported by the National Key R&D Program of China (022YFC2505100, 2022YFC2304900); Outstanding Young Scholars Support Program (3111500001); Xi'anJiaotong University Basic Research and Profession Grant (xtr022019003, xzy032020032) and Xi'an Jiaotong University Young Scholar Support Grant (YX6J004). M.Y. is supported by the Melbourne Research Scholarship established by the University of Melbourne. The funding source had no role in the design and conduct of the study; collection, management, analysis, and interpretation of the data; preparation, review, or approval of the manuscript; and decision to submit the manuscript for publication.

Disclosure: **M. Yusufu**, None; **M. Kang**, None; **A. Dayimu**, None; **D. Shi**, None; **L.Z. Zhu**, None; **R. Chen**, None; **A.J. Vingrys**, None; **X. Shang**, None; **M. He**, None; **L. Zhang,** None

References

1. Australian Institute of Health and Welfare. (2023). Deaths in Australia. Available from: https://www.aihw.gov.au/reports/life-expectancy-death/deaths-in-australia. Accessed July 27, 2023.
2. Rhodes HG, ed. *Measuring the Risks and Causes of Premature Death: Summary of Workshops*. Washington: National Academies Press; 2015.
3. Stringhini S, Carmeli C, Jokela M, et al. Socioeconomic status and the 25 × 25 risk factors as determinants of premature mortality: a multicohort study and meta-analysis of 1·7 million men and women. *Lancet*. 2017;389(10075):1229–1237.
4. Bérard E, Bongard V, Arveiler D, et al. Ten-year risk of all-cause mortality: assessment of a risk prediction algorithm in a French general population. *Eur J Epidemiol*. 2011;26:359–368.
5. Ganna A, Ingelsson E. 5 year mortality predictors in 498,103 UK Biobank participants: a prospective population-based study. *Lancet*. 2015;386(9993):533–540.
6. Loprinzi PD, Addoh O. Predictive validity of the American College of Cardiology/American Heart Association pooled cohort equations in predicting all-cause and cardiovascular disease-specific

mortality in a national prospective cohort study of adults in the United States. *Mayo Clin Proc*. 2016;91:763–769.
7. Mangold C, Zoretic S, Thallapureddy K, Moreira A, Chorath K, Moreira A. Machine learning models for predicting neonatal mortality: a systematic review. *Neonatology*. 2021;118:394–405.
8. Wang YX, Mínguez-Alarcón L, Gaskins AJ, et al. Association of spontaneous abortion with all cause and cause specific premature mortality: prospective cohort study. *BMJ*. 2021;372:n530.
9. Chen Y, Freedman ND, Albert PS, et al. Association of cardiovascular disease with premature mortality in the United States. *JAMA Cardiol*. 2019;4:1230–1238.
10. Sun Y, Yu Y, Zhang K, et al. Association between Life's Essential 8 score and risk of premature mortality in people with and without type 2 diabetes: A prospective cohort study. *Diabetes Metab Res Rev*. 2023;39(5):e3636.
11. Chen C, Ye Y, Zhang Y, Pan XF, Pan A. Weight change across adulthood in relation to all cause and cause specific mortality: prospective cohort study. *BMJ*. 2019;367:l5584.
12. Minakaran N, de Carvalho ER, Petzold A, Wong SH. Optical coherence tomography (OCT) in neuro-ophthalmology. *Eye*. 2021;35:17–32.
13. Liu YL, Hsieh YT, Chen TF, et al. Retinal ganglion cell-inner plexiform layer thickness is nonlinearly associated with cognitive impairment in the community-dwelling elderly. *Alzheimers Dement*. 2019;11:19–27.
14. López-de-Eguileta A, Cerveró A, Ruiz de Sabando A, Sánchez-Juan P, Casado A. Ganglion cell layer thinning in Alzheimer's disease. *Medicina*. 2020;56:553.
15. Mysore N, Koenekoop J, Li S, et al. A review of secondary photoreceptor degenerations in systemic disease. *Cold Spring Harb Perspect Med*. 2014;5(11):a025825.
16. von Elm E, Altman DG, Egger M, Pocock SJ, Gøtzsche PC, Vandenbroucke JP. The Strengthening the Reporting of Observational Studies in Epidemiology (STROBE) statement: guidelines for reporting observational studies. *Lancet*. 2007;370(9596):1453–1457.
17. Sudlow C, Gallacher J, Allen N, et al. UK Biobank: an open access resource for identifying the causes of a wide range of complex diseases of middle and old age. *PLoS Med*. 2015;12(3):e1001779.
18. Chua SYL, Thomas D, Allen N, et al. Cohort profile: design and methods in the eye and vision consortium of UK Biobank. *BMJ Open*. 2019;9(2):e025077.
19. Liew G, Mitchell P, Rochtchina E, et al. Fractal analysis of retinal microvasculature and coronary heart disease mortality. *Eur Heart J*. 2011;32:422–429.
20. Yang Q, Reisman CA, Wang Z, et al. Automated layer segmentation of macular OCT images using dual-scale gradient information. *Opt Express*. 2010;18:21293–21307.
21. Patel PJ, Foster PJ, Grossi CM, et al. Spectral-domain optical coherence tomography imaging in 67 321 adults: associations with macular thickness in the UK Biobank Study. *Ophthalmology*. 2016;123:829–840.
22. Ko F, Foster PJ, Strouthidis NG, et al. Associations with retinal pigment epithelium thickness measures in a large cohort: results from the UK Biobank. *Ophthalmology*. 2017;124:105–117.
23. Liu J, Chen Y, Lu X, et al. The association between dietary iron intake and incidence of dementia in adults aged 60 years or over in the UK Biobank. *Nutrients*. 2023;15:260.
24. Timmers P, Wilson JF, Joshi PK, Deelen J. Multivariate genomic scan implicates novel loci and haem metabolism in human ageing. *Nat Commun*. 2020;11(1):3570.
25. Lin Q, Jia Y, Li T, et al. Optic disc morphology and peripapillary atrophic changes in diabetic children and adults without diabetic retinopathy or visual impairment. *Acta Ophthalmol*. 2022;100(1):e157–e166.
26. Hirooka K, Oki K, Ogawa-Ochiai K, Nakaniida Y, Onoe H, Kiuchi Y. Blood flow in the optic nerve head in patients with primary aldosteronism. *PLoS One*. 2023;18(4):e0285039.
27. Lim HB, Shin YI, Lee MW, Koo H, Lee WH, Kim JY. Ganglion cell - inner plexiform layer damage in diabetic patients: 3-year prospective, longitudinal, observational study. *Sci Rep*. 2020;10(1):1470.
28. Horstmann L, Schmid H, Heinen AP, Kurschus FC, Dick HB, Joachim SC. Inflammatory demyelination induces glia alterations and ganglion cell loss in the retina of an experimental autoimmune encephalomyelitis model. *J Neuroinflammation*. 2013;10:120.
29. Chua SYL, Dhillon B, Aslam T, et al. Associations with photoreceptor thickness measures in the UK Biobank. *Sci Rep*. 2019;9(1):19440.
30. Chua SYL, Welsh P, Sun Z, et al. Associations between HbA1c across the normal range, diagnosed, and undiagnosed diabetes and retinal layer thickness in UK Biobank Cohort. *Transl Vis Sci Technol*. 2023;12(2):25.

31. Harris J, Subhi Y, Sørensen TL. Effect of aging and lifestyle on photoreceptors and retinal pigment epithelium: cross-sectional study in a healthy Danish population. *Pathobiol Aging Age Relat Dis*. 2017;7(1):1398016.
32. Lim HB, Lee MW, Park JH, Kim K, Jo YJ, Kim JY. Changes in ganglion cell-inner plexiform layer thickness and retinal microvasculature in hypertension: an optical coherence tomography angiography study. *Am J Ophthalmol*. 2019;199:167–176.
33. Kergoat H, Hérard ME, Lemay M. RGC sensitivity to mild systemic hypoxia. *Invest Ophthalmol Vis Sci*. 2006;47:5423–5427.
34. Scarinci F, Jampol LM, Linsenmeier RA, Fawzi AA. Association of diabetic macular nonperfusion with outer retinal disruption on optical coherence tomography. *JAMA Ophthalmol*. 2015;133:1036–1044.
35. Pedersen BK, Febbraio MA. Muscles, exercise and obesity: skeletal muscle as a secretory organ. *Nat Rev Endocrinol*. 2012;8:457–465.
36. Walsh NP, Gleeson M, Shephard RJ, et al. Position statement. Part one: Immune function and exercise. *Exerc Immunol Rev*. 2011;17:6–63.
37. Kim CS, Park S, Chun Y, Song W, Kim HJ, Kim J. Treadmill exercise attenuates retinal oxidative stress in naturally-aged mice: an immunohistochemical study. *Int J Mol Sci*. 2015;16:21008–21020.
38. Ozkaya A, Alkin Z, Karakucuk Y, et al. Thickness of the retinal photoreceptor outer segment layer in healthy volunteers and in patients with diabetes mellitus without retinopathy, diabetic retinopathy, or diabetic macular edema. *Saudi J Ophthalmol*. 2017;31:69–75.
39. Faria A, Persaud SJ. Cardiac oxidative stress in diabetes: mechanisms and therapeutic potential. *Pharmacol Ther*. 2017;172:50–62.
40. Marques CMS, Nunes EA, Lago L, et al. Generation of advanced glycation end-products (AGEs) by glycoxidation mediated by copper and ROS in a human serum albumin (HSA) model peptide: reaction mechanism and damage in motor neuron cells. *Mutat Res Genet Toxicol Environ Mutagen*. 2017;824:42–51.
41. Nakayama M, Iejima D, Akahori M, Kamei J, Goto A, Iwata T. Overexpression of HtrA1 and exposure to mainstream cigarette smoke leads to choroidal neovascularization and subretinal deposits in aged mice. *Invest Ophthalmol Vis Sci*. 2014;55:6514–6523.
42. Jager RD, Mieler WF, Miller JW. Age-related macular degeneration. *N Engl J Med*. 2008;358:2606–2617.
43. McFarland RA, Fisher MB. Alterations in dark adaptation as a function of age. *J Gerontol*. 1955;10:424–428.
44. Ogburn-Russell L, Johnson JE. Oxygen saturation levels in the well elderly: altitude makes a difference. *J Gerontol Nurs*. 1990;16(10):26–30.
45. Goerdt L, Swain TA, Kar D, et al. Band visibility in high-resolution optical coherence tomography assessed with a custom review tool and updated, histology-derived nomenclature. *Transl Vis Sci Technol*. 2024;13(12):19.
46. Lange CA, Bainbridge JW. Oxygen sensing in retinal health and disease. *Ophthalmologica*. 2012;227:115–131.
47. Curcio CA, Kar D, Owsley C, Sloan KR, Ach T. Age-related macular degeneration, a mathematically tractable disease. *Invest Ophthalmol Vis Sci*. 2024;65(3):4.
48. Ehrlich JR, Ramke J, Macleod D, et al. Association between vision impairment and mortality: a systematic review and meta-analysis. *Lancet Glob Health*. 2021;9(4):e418–e430.
49. Deák GG, Schmidt-Erfurth UM, Jampol LM. Correlation of central retinal thickness and visual acuity in diabetic macular edema. *JAMA Ophthalmol*. 2018;136:1215–1216.